

Efficient Temporal Extrapolation of Multimodal Large Language Models with Temporal Grounding Bridge

Anonymous ACL submission

Abstract

Despite progress in multimodal large language models (MLLMs), the challenge of interpreting long-form videos in response to linguistic queries persists, largely due to the inefficiency in temporal grounding and limited pre-trained context window size. In this work, we introduce Temporal Grounding Bridge (TGB), a novel framework that bootstraps MLLMs with advanced temporal grounding capabilities and broadens their contextual scope. Our framework significantly enhances the temporal capabilities of current MLLMs through three key innovations: an efficient multi-span temporal grounding algorithm applied to low-dimension temporal features projected from flow; a multi-modal length extrapolation training paradigm that utilizes low-dimension temporal features to extend the training context window size; and a bootstrapping framework that bridges our model with pluggable MLLMs without requiring annotation. We validate TGB across seven video benchmarks and demonstrate substantial performance improvements compared with prior MLLMs. Notably, our model, initially trained on sequences of four frames, effectively handles sequences up to $16\times$ longer without sacrificing performance, highlighting its scalability and effectiveness in real-world applications. Our code is publicly available.

1 Introduction

A fundamental aspect of human intelligence is to effortlessly perceive, memorize, and comprehend daily multi-modal information such as events, observations, and videos that span hours and days. Such capacity of long-form multi-modal understanding, seamlessly integrating prolonged visual dynamics with textual cues, poses considerable challenges for contemporary machine perceptual systems. A wide range of research works in computer vision and multi-modal tasks has extensively delved into real-life videos, including video question answering (VideoQA) (Yu et al., 2018, 2019),

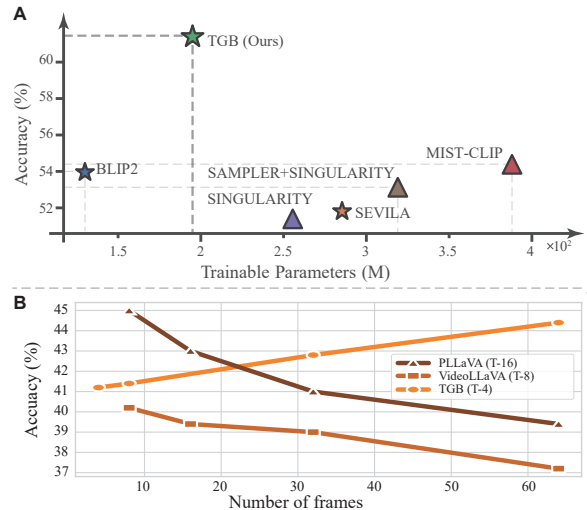


Figure 1: Training Efficiency and Length Extrapolation of TGB. **A.** Our method demonstrates the best performance with less trainable parameters. **B.** Results of frame extrapolation on EgoSchema (Mangalam et al., 2023) under zero-shot setting. $T\text{-}num$ indicates the number of training context window size. By training with four-frame videos, our model shows consistent performance on extended video length.

text-to-video retrieval (Hendricks et al., 2017), video captioning (Xu et al., 2016; Krishna et al., 2017), *etc.* Despite the prominent advancements in many video-language benchmarks (Yu et al., 2018, 2019; Hendricks et al., 2017; Xu et al., 2016; Krishna et al., 2017), understanding long-form videos with task-oriented linguistic queries still suffers from the significant computational overhead (Buch et al., 2022; Gao et al., 2023a; Yu et al., 2023; Song et al., 2023; He et al., 2024) imposed by high-dimensional video data and the disparity between language and spatial-temporal visual cues (Lei et al., 2022; Xiao et al., 2023a).

Some researchers have proposed scaling up the amount of vision data fed into larger models (Bai et al., 2023; Liu et al., 2024a), following the scaling law observed in LLMs. However,

060 the scarcity of high-quality, long video-language
061 datasets makes this approach difficult. Others have
062 explored sampling-based methods to reduce input
063 overhead by selecting relevant frames at either the
064 frame level (Lei et al., 2021; Wang et al., 2023; Bain
065 et al., 2021; Buch et al., 2022) or token level (Gao
066 et al., 2023a). These methods have three main lim-
067 itations: first, they are computationally inefficient
068 with slow training and inference speeds due to
069 the large number of tunable parameters; second,
070 the sampling strategy may miss important motion
071 features, especially when there’s misalignment be-
072 tween the video segment and the language query;
073 and third, the complexity of the specialized vision
074 encoder complicates the adaptation to long-video
075 understanding.

076 To address these challenges, we present a novel
077 framework, Temporal Grounding Bridge, which
078 enriches image-language models with temporal pri-
079 ors, significantly improving the understanding of
080 long videos. TGB distinguishes itself in the follow-
081 ing key aspects:

082 **Efficient and Adaptable Video Compression:**
083 TGB features a Bridge that is both lightweight and
084 adaptable. To achieve this, we introduce a learnable
085 multi-span algorithm capable of simultaneously
086 extracting multiple relevant segments from low-
087 dimension motion features. Subsequently, we can
088 compress the entire video into several keyframes.
089 This method efficiently balances performance and
090 resource consumption when processing long-form
091 videos, as demonstrated by our results on the
092 AGQA (Grunde-McLaughlin et al., 2021), with a
093 relatively low parameter count (see Fig. 1A).

094 **Temporal Extrapolation Preserving Motion**
095 **Features:** A significant advantage of the TGB
096 lies in its ability to preserve the continuity of video
097 content, thereby maintaining the temporal dynam-
098 ics discarded by previously extracted keyframes. To
099 achieve this, we retain the low-dimensional motion
100 features extracted by the TGB to supplement these
101 keyframes. Additionally, we utilize extrapolative
102 position encoding to ensure that these features re-
103 main extendable. This approach allows our method
104 to extrapolate to longer sequences in a zero-shot
105 setting (see Fig. 1B).

106 **Bootstrapping Framework without Annota-**
107 **tion:** Due to the high cost of manual annota-
108 tions and the limited availability of video data
109 compared to image data, we developed a frame-
110 work that leverages MLLMs without requiring
111 them to be pretrained on videos. Our approach em-

112 ploys a bootstrapping strategy to refine TGB using
113 MLLMs, eliminating the need for explicit temporal
114 grounding annotations. This strategy also allows
115 for joint training with MLLMs by incorporating the
116 Gumbel-Softmax trick. Additionally, our bootstrap-
117 ping framework, when integrated with the afore-
118 mentioned mechanism, can be trained on standard
119 video data and still achieve strong performance on
120 much longer sequences (see Fig. 1B).

121 To validate the effectiveness of TGB, we con-
122 ducted experiments on long-form video question
123 answering with seven datasets: AGQA 2.0 (Grunde-
124 McLaughlin et al., 2021), NExT-QA (Xiao et al.,
125 2021), Egoschema (Mangalam et al., 2023),
126 MSVD (Xu et al., 2017), MSRVT (Xu et al.,
127 2016), and ActivityNet (Yu et al., 2019). Ad-
128 ditionally, we tested temporal question ground-
129 ing on video using the NExT-GQA dataset (Xiao
130 et al., 2023a). Consistent improvements across
131 these datasets confirm the efficacy of our approach.
132 TGB has shown strong generalization capabili-
133 ties across five MLLMs (across encoder, encoder-
134 decoder, and decoder-only) and two LLMs. Further
135 enhancements include the incorporation of a gen-
136 eral multimodal instruction-tuning dataset, which
137 shows promise for video chat agent applications. In
138 comparison to other leading-edge methods, TGB
139 provides substantial efficiency and efficacy bene-
140 fits.

141 2 Related Work

142 **Long-form Video Understanding** The com-
143 putational demands of processing long-form videos
144 have led to research exploring various methods
145 to address the challenge. A common approach in-
146 volves sampling-based techniques that aim to re-
147 duce the computational load by selectively choos-
148 ing relevant frames. Research (Lei et al., 2021;
149 Wang et al., 2023; Bain et al., 2021) integrate sparse
150 sampling within the framework of video-language
151 pretraining. (Buch et al., 2022) introduce an atem-
152 poral probe (ATP) model that seeks to distill a sin-
153 gle image representation from a video clip for more
154 details. Despite these advancements, there’s a risk
155 that sparse sampling may lead to an insufficient
156 representation of visual information, which may
157 not be relevant to corresponding language queries.
158 MIST (Gao et al., 2023a) attempts to address this
159 by leveraging the inherent structure of videos to
160 iteratively select and sample spatial-temporal infor-
161 mation within a Transformer architecture. Nonethe-

less, these methods often suffer from reduced computational efficiency and prolonged training and inference times due to the extensive tunable parameters required for processing either spatial or temporal dimensions. More recent studies are exploring the utilization of LLMs for enhancing long-form video understanding. These approaches include a range of techniques such as incorporating temporal embeddings (Qian et al., 2024), applying prompt-based strategies (Yu et al., 2023; Ren et al., 2023), condensing video frames through a similarity metric (Song et al., 2023), compressing visual tokens with resampling methods (Korbar et al., 2023; Ma et al., 2023; Liu et al., 2024b), and employing retrieval-based methods that integrate visual features (He et al., 2024). To overcome the constraints of current methods, which usually depend on human-provided annotations for time alignment or require intricate encoding of context, our proposed approach employs a novel bootstrapping framework. This framework enhances a temporal grounding bridge, using MLLMs. This bridge is designed to simultaneously capture multiple granular pieces of key information by leveraging multi-span sampling, which it then integrates with low-dimensional motion features for a more efficient and effective representation.

Bootstrapping Large Language Models for Visual Tasks Capitalizing on the success of large language models (LLMs) in NLP, there is a growing trend of applying them to computer vision tasks, such as VQA (Lu et al., 2022; Chen et al., 2023; Fu et al., 2023; Liu et al., 2023b; Li et al., 2023a), image generation (Ku et al., 2023; Zhang et al., 2023b), and visual instruction following (Xu et al., 2022; Li et al., 2023c). The research mainly progresses along three avenues: (i) leveraging LLMs’ reasoning for visual tasks (Huang et al., 2023; Wu et al., 2023; Driess et al., 2023; Surís et al., 2023); (ii) adapting Transformer or linear networks to equip LLMs with visual perception (Li et al., 2023b; Dai et al., 2023; Zhu et al., 2023; Xu et al., 2023; Gao et al., 2023b; Liu et al., 2023a); (iii) merging LLMs with video and audio inputs (Zhang et al., 2023a; Maaz et al., 2023; Lyu et al., 2023). Recently, Sevilla’s (Yu et al., 2023) self-chained VideoQA framework uses a two-step approach: selecting keyframes with a tailored prompt and applying them to tasks. However, it faces three issues: time-consuming keyframe localization, static frames missing motion details, and incomplete video representation by sampled

frames. Addressing these, we introduce a TGB that incorporates both static and dynamic features for video-language understanding.

3 Methodology

In the subsequent sections, we begin with a detailed formulation of the video-language understanding problem in Section §3.1. Next, in Section §3.2, we outline the core components for efficient length extrapolation of our TGB. Section §3.3 explains the process of jointly tuning TGB with pluggable MLLMs on new video-language datasets within our Bootstrapping framework. The overall architecture of TGB is illustrated in Figure 2.

3.1 Problem Definition

We formalize the open-ended video-text understanding problem. The input video V is denoted as a sequence of image frames $V = \{fr_1, fr_2, \dots, fr_T\}$, where T is the total number of frames. The input language L , denoted as a sequence of N tokens starting with [CLS], is a task-relevant prompt or question related to interactions among objects, relationships, or events that occur within a few frames of the video. Our goal is to identify the keyframes that relate to the query as grounded moments and generate an open-ended answer in the form of natural language response y , incorporating time priors. In the following sections, we use $f(\cdot)$ to indicate trainable parameters or neural networks and $\tilde{f}(\cdot)$ to indicate frozen pre-trained models.

3.2 Temporal Grounding Bridge

Previous Video-Language Understanding models commonly extract temporal features from video-text data using offline video encoders or image encoders (Carreira and Zisserman, 2017; Jiang et al., 2017; Xie et al., 2017; Feichtenhofer et al., 2019; Liu et al., 2021a; Tong et al., 2022), causing the model to be time-consuming and lack generality. To address these limitations, we propose a novel mechanism that combines high-dimension key visual cues with low-dimension motion features, ensuring efficiency without compromising visual information. We further contend that temporal grounding does not necessitate dense frame-level features. To support this claim, we introduce a Temporal Grounding Bridge that incorporates optical flows (Jiang et al., 2019; Feichtenhofer et al., 2019; Pfister et al., 2015; Feng et al., 2023; Zhang et al., 2018) during the temporal grounding

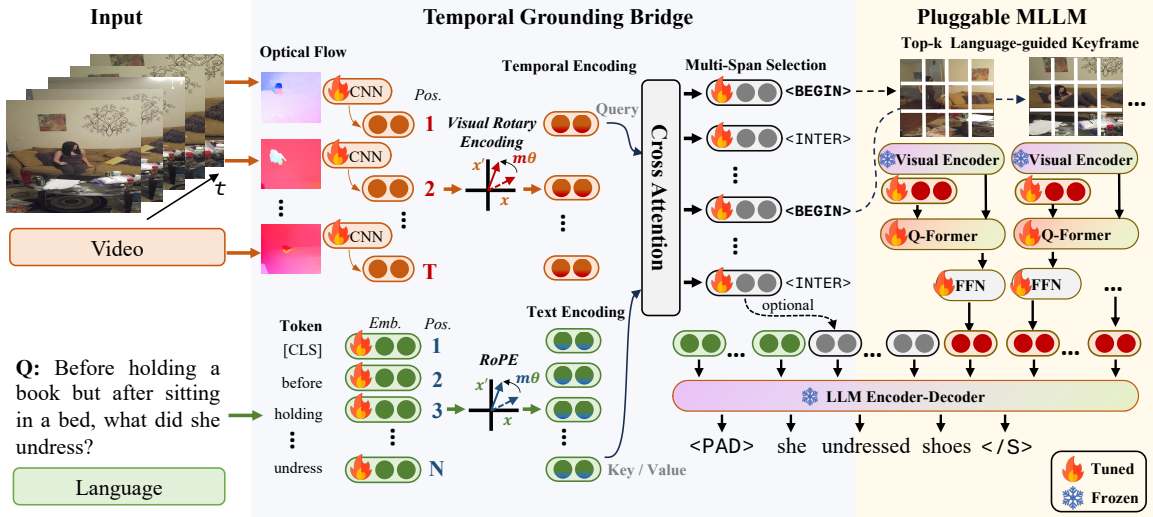


Figure 2: **Overview of TGB framework (BLIP-based).** The Temporal Grounding Bridge (§3.2) is designed to capture temporal priors as well as the specific moments in a video that are grounded by language. We further develop a pluggable bootstrapping framework (§3.3) that incorporates TGB-MLLM alignment, utilizing a joint optimization strategy.

stage through a dimensionality reduction. By injecting language queries, this approach generates parameter-efficient, language-guided temporal features. **A key distinction of our work is that we do not use optical flow merely as supplementary information to enhance frame-based performance. Instead, our framework employs flow as a low-dimensional bridge, which can be directly or indirectly applied to infuse motion details into MLLMs. Importantly, the flow feature can be substituted with other types of features if needed.**

Feature Extraction We denote the optical flow for each pair of video frames as $OF = \{of_1, of_2, \dots, of_T\}$. The low-dimensional visual encoding is then computed over these extracted optical flows with a simple convolutional layer followed by a multi-layer perceptron (MLP) $E_{of} = \text{MLP}(\text{CNN}(of))$. For language queries, we use a trainable embedding layer to represent the soft query prompt, *i.e.*, $E_l = \text{Embedding}(Q)$, where Q is the language query.

Temporal Feature Length Extrapolation Despite the impressive efficacy of Transformer-based models within the sphere of deep learning, their operational capacity is inherently constrained by the length of the input. In the context of our research, the bridge is meticulously devised to identify the most salient portions of an entire video, the duration of which may potentially exceed the predetermined limit and differ significantly across various

instances. Current literature employs a sampling strategy to condense the video, a process that unfortunately results in the loss of substantial temporal information inherent in the video. To mitigate this challenge, inspired by rotary position embedding (RoPE) (Su et al., 2021), we add multimodal extrapolative position encoding to our TGB (Fig. 2). Specifically, we compute the position-encoded features using RoPE mechanism for each optical flow and language token, respectively. Formally, the position-encoded features can be denoted as

$$\begin{aligned} E_{of}^R &= \text{RoPE}(W_{of}E_{of}, Pos_{of}), \\ E_l^R &= \text{RoPE}(W_lE_l, Pos_l), \end{aligned} \quad (1)$$

where W_{of}, W_l are transformation matrices, Pos_{of}, Pos_l are corresponding position indices of OF and L .

Given the temporal features, we adopt the cross-attention (Vaswani et al., 2017) mechanism, which is computed using optical flow rotary encoding as query $\mathbf{Q}_R = E_{of}^R$, rotary language embedding as key $\mathbf{K}_R = E_l^R$, and language embedding as value $\mathbf{V} = W_V E_l$.

The final language-guided temporal feature E_R is calculated by the standard cross-attention mechanism, *i.e.*, $E_R = \text{Softmax}\left(\frac{\mathbf{Q}_R \mathbf{K}_R^T}{\sqrt{d_k}}\right) \mathbf{V}$.

Multi-Span Keyframe Selection Based on the flow-language encoding, we formulate the temporal question grounding video task as multi-span reading comprehension (RC) problem, where an

RC head is to predict the label of fused encoding $\{e_{R1}, e_{R2}, \dots, e_{RT}\}$ as one of {"<BEGIN>", "<END>", "<NONE>"} of the grounded video spans. The selection can be formulated as:

$$h = \mathcal{F}_\theta(e_{R1}, e_{R2}, \dots, e_{RT}), \quad (2)$$

$$index = \arg \max(\text{Softmax}(h)),$$

where \mathcal{F}_θ denotes the RC head for span selection, $index$ is the prediction of the start or end index. The objective is computed as the cross-entropy between the prediction and pseudo labels. During Inference, we can obtain an arbitrary number of k segments of grounded video by predicting k <BEGIN> s and k <END> s with the RC Head. Finally, we union these segments to eliminate the overlap between these extracted spans. **Appendix D** demonstrates commonly used methods for temporal sentence grounding on video tasks. Compared with other span-fixed methods, our method could obtain multiple grounded video spans with the least time complexity and space complexity.

Bridge with MLLMs For each selected keyframe fr_k , we utilize a frozen pre-trained visual encoder to capture its spatial information, *i.e.*, $E_{fr} = \text{Enc}_v(fr_k)$. In line with contemporary research, we adapt the visual feature via a pre-trained Q-former and obtain q query representations. $\tilde{E}_q = \text{Enc}_q(E_q, E_{fr})$, where E_q represents the learnable query, $\tilde{E}_q = \{e_q\}$ is the spatial visual feature output of the MLLM. The final output is produced by feeding obtained spatial-temporal-language information in to a frozen LLM, *i.e.*, $y = \text{LLM}(E_r, \tilde{E}_q, E_l)$.

3.3 Joint Training Bootstrapping Framework

Bootstrapping Algorithm Due to the scarcity of video-language datasets with temporally grounded annotations and the high cost of acquiring human labeling, we have developed a self-improvement algorithm to enhance TGB using the capabilities of MLLM. There are two primary types of video-language understanding tasks: close-ended and open-ended. We have tailored algorithms to address both types. For close-ended tasks, we employ an iterative method in which each video frame is evaluated using the MLLM. Frames that lead to correct MLLM predictions are marked with positive labels, while those with incorrect predictions receive negative labels. For open-ended tasks, which often lack temporal labels, we introduce an innovative approach to generate pseudo labels

for open-ended datasets. We analyze the MLLM-generated results of uniformly sampled frames and compute the sentence similarity between these results and the ground truth. We then apply a monotonic stack algorithm to identify the span with the highest similarity scores. These pseudo labels are used to optimize the TGB. Detailed information about the this algorithm can be found in the **Appendix A**.

Joint Optimization Despite the utilization of pseudo labels in the training process, in many videos, there is implicit alignment between query and videos. In addition, the fixation of the pre-trained bridge within the bootstrapping framework inevitably leads to the introduction of exposure bias. To mitigate this we suggest a joint training approach that extends the Gumbel-Softmax technique. We implement Gumbel-Softmax sampling K times to sample K spans:

$$\text{GumbelSoftmax}(\mathcal{F}_\theta(e_{R1}, \dots, e_{RT}), \tau), \quad (3)$$

where τ is the scaling term for reparameterizing. Consequently, our methodology is employed to facilitate a connection between TGB and MLLMs, thereby enabling our framework to be jointly optimized on domain-specific datasets.

4 Experiments

In this section, we utilize the TGB on 5 MLLMs, across encoder, encoder-decoder, and decoder-only three types of architectures. We demonstrate the effectiveness of our approach on three tasks: long-form videoQA and zero-shot open-domain videoQA (Section 4.1), temporal question grounding on video (Section 4.2). Furthermore, We provide a detailed analysis to showcase the effectiveness of our framework in length extrapolation (Fig. 1B), the effectiveness of different components (Section 4.3), and compare its computational efficiency with other state-of-the-art models on a similar scale (Section 4.4).

4.1 Long-form Video Question Answering

Setups We take three long-form VideoQA benchmarks AGQA (Grunde-McLaughlin et al., 2021), NExTQA (Xiao et al., 2021), and EgoSchema (Mangalam et al., 2023) for evaluation. We use two types of baselines: retrieval-based models and open-ended models focusing on recent SOTA temporal priors learning models for comparative analysis. For the retrieval-based models, in

Model	Object-relation	Relation-action	Object-action	Superlative	Sequencing	Exists	Duration comparison	Action recognition	Overall
<i>Retrieval-based Video-Language Models</i>									
HME (Fan et al., 2019)	37.42	49.90	49.97	33.21	49.77	49.96	47.03	5.43	39.89
PSAC (Li et al., 2019)	37.84	49.95	50.00	33.20	49.78	49.94	45.21	4.14	40.18
HCRN (Le et al., 2020)	40.33	49.86	49.85	33.55	49.70	50.01	43.84	5.52	42.11
AIO (Wang et al., 2023)	48.34	48.99	49.66	37.53	49.61	50.81	45.36	18.97	48.59
ATP (Buch et al., 2022)	50.15	49.76	46.25	39.78	48.25	51.79	49.59	18.96	49.79
MIST-AIO (Gao et al., 2023a)	51.43	54.67	55.37	41.34	53.14	53.49	47.48	20.18	50.96
ALBEF	50.53	49.39	49.97	38.22	49.79	54.11	48.01	10.40	50.68
ALBEF + TGB (Ours)	51.05	51.11	51.66	38.36	51.33	58.10	49.20	11.78	51.73
SINGULARITY (Lei et al., 2022)	50.87	50.67	49.70	40.47	40.79	55.34	48.20	11.59	51.11
SINGULARITY + TGB (Ours)	52.33	54.12	55.07	40.71	54.49	57.88	48.35	12.24	53.13
VIOLET (Fu et al., 2021)	50.89	50.24	50.93	40.76	50.51	58.07	38.97	6.53	51.03
VIOLET + TGB (Ours)	51.59	54.54	56.96	40.94	55.61	59.12	42.81	9.02	52.59
<i>Open-ended Video-Language Models</i>									
SeViLA* (Yu et al., 2023)	51.15	48.93	62.08	42.24	55.96	53.02	38.91	0.00	51.70
BLIP2 (Li et al., 2023b)	53.72	48.64	62.1	43.84	55.94	55.14	40.39	0.28	54.00
TGB-BLIP2 (Ours)	62.27	51.74	66.09	53.67	60.11	60.85	36.99	0.00	61.45

* Re-implementation result. We removed prior information from QVHighlights (Lei et al.) used in SeViLA for fair comparison.

Table 1: Comparison accuracy of different sampling-based SOTA models on AGQA 2.0.

Model	Temporal	Causal	Description	All
<i>Retrieval-based Video-Language Models</i>				
CLIP (Radford et al., 2021)	46.3	39.0	53.1	43.7
HGA (Jiang and Han, 2020)	44.2	52.5	44.1	49.7
AIO (Wang et al., 2023)	48.0	48.6	63.2	50.6
VQA-T (Yang et al., 2021)	49.6	51.5	63.2	52.3
MIST-AIO (Gao et al., 2023a)	51.6	51.5	64.2	53.5
ATP (Buch et al., 2022)	50.2	53.1	66.8	54.3
VGT (Xiao et al., 2022)	52.3	55.1	64.1	55.0
MIST-CLIP (Gao et al., 2023a)	56.6	54.6	66.9	57.1
<i>Open-ended Video-Language Models</i>				
BLIP2 (Li et al., 2023b)	64.9	69.7	79.4	69.6
SeViLA* (Yu et al., 2023)	66.4	71.9	80.8	71.5
TGB-BLIP2 (Ours)	66.5	72.8	81.2	72.1

* We removed prior information from QVHighlights used in SeViLA for fair comparison.

Table 2: Comparison accuracy of long-form video QA on NExT-QA.

addition to traditional methods (Fan et al., 2019; Li et al., 2019; Le et al., 2020; Wang et al., 2023; Li et al., 2021; Lei et al., 2022; Fu et al., 2021), we use recent SOTA temporal learning models, specifically ATP (Buch et al., 2022) and MIST (Gao et al., 2023a). For the open-ended models, we use BLIP2 (Li et al., 2023b) and SEVILA (Yu et al., 2023). For the number of keyframes, we sample 4 frames for TGB and 6 frames for TGB-augmented methods (where we don’t incorporate the motion feature to the input directly) in all experiments. For more implementation details, please refer to **Appendix F.1**.

Results on AGQA 2.0 Our TGB framework, compared with prior works that integrate keyframe localization into video-language tasks, shows that BLIP2, despite its 4.1B parameters pre-trained on 129M images, offers only a slight improvement over smaller models, as demonstrated in AGQA

Methods	Base Model	# of Frames	Accuracy
Sevila	BLIP2	32	25.7
mPLUG-Owl	LLaMA-7b	5	33.8
Video-LLaVA	LLaVA-7b	8	40.2
TGB-BLIP2	BLIP2	4	41.2

Table 3: Zero-shot Result on subset of EgoSchema

2.0 results. BLIP2 even falls short of the state-of-the-art MIST-CLIP, which has a parameter count comparable to BERT (Devlin et al., 2019). This indicates that simply adapting videos for LLMs is inadequate for complex video question-answering tasks. However, when enhanced with our TGB framework, BLIP2’s accuracy increases by 7.45 points, underscoring the framework’s ability to learn spatial-temporal video features effectively. We believe this is due to our framework’s superior temporal information capture, which other methods miss. Nonetheless, it still lags behind MIST-CLIP on certain question types, stemming from the inherent differences in how retrieval-based and open-ended models produce answers. For example, open-ended models struggle with “Duration comparison” questions because they are limited to generating answers from a specific set of 171 words or phrases, which are infrequently found in generative models’ pre-training data, posing a challenge for exact match generation.

Results on NExTQA Table 2 presents the results on the NExTQA dataset. Generally, our method outperforms a variety of baselines, particularly SeViLA, a recent model using LLM for keyframe selection. However, the performance im-

Methods	LLM size	MSVD-QA		MSRVTT-QA		ActivityNet-QA	
		Accuracy	Score	Accuracy	Score	Accuracy	Score
FrozenBiLM	1B	32.2	-	16.8	-	24.7	-
VideoChat	7B	56.3	2.8	45.0	2.5	-	2.2
LLaMA-Adapter	7B	54.9	3.1	43.8	2.7	34.2	2.7
Video-LLaMA	7B	51.6	2.5	29.6	1.8	12.4	1.1
Video-ChatGPT	7B	64.9	3.3	49.3	2.8	35.2	2.7
TGB (BLIP2)	3B	66.0	3.6	53.5	3.1	41.3	3.1
TGB (Vicuna7B)	7B	71.4	3.9	57.3	3.3	43.9	3.3

Table 4: Zero-shot Open Domain Video QA.

465 improvement of our framework on NEXTQA is not as
466 significant as on AGQA. This is because NEXTQA
467 places more emphasis on causality, and videos in
468 NEXTQA, sourced from VidOR (Shang et al., 2019;
469 Thomee et al., 2016), a dataset focused on video ob-
470 jects and relation recognition, exhibit more "static
471 appearance bias" (Lei et al., 2022) than AGQA.

472 **Results on EgoSchema** We evaluated our
473 model’s performance on the EgoSchema (Man-
474 galam et al., 2023), one of the longest videoQA
475 datasets available. We apply this experiment un-
476 der the zero-shot setting, thereby trained on video
477 instruction dataset from VideoLLaVA (Lin et al.,
478 2023). As shown in Table 3, our model outperforms
479 other models that use similar pretraining data. This
480 superior performance is particularly notable given
481 that our base model is smaller and processes fewer
482 input instances compared to the others. We believe
483 our approach is highly effective for understanding
484 long-form video content.

485 **Impact of TGB-grounded frames** We as-
486 sessed the influence of TGB on different MLLMs
487 by testing them with alternative MLLMs and TGB-
488 grounded frames, excluding optical flow features.
489 For MLLMs using single-image input, we merged
490 multiple images using an early fusion approach.
491 Our experiments on the AGQA 2.0 dataset in Ta-
492 ble 1 revealed: ❶ *TGB matters in temporal learn-*
493 *ing over different MLLMs.* TGB-augmented meth-
494 ods significantly enhances MLLMs’ ability in solv-
495 ing temporal question (*i.e.*, “Relation-action
496 ”, “Sequencing”, “Exists”) compared to the
497 uniform sampling strategy. ❷ *Absence in temporal*
498 *priors hinders the performance of ensemble meth-*
499 *ods.* The improvement gained on SINGULARITY
500 is better than ALBEF, despite they have similar
501 objectives but SINGULARITY is pre-trained with
502 video corpora. ❸ *Temporal features of optical flow*
503 *can compensate for the information loss caused*
504 *by frame sampling.* The marginal improvement of
505 our TGB-augmented models on “Superlative”
506 suggests that the sampling strategy cannot enhance
507 the model’s overall video understanding ability. In
508 contrast, our BLIP2-based framework with opti-

Method	Vision Encoder	mIoU	IoU@0.3	IoU@0.5
VGT	RCNN	3.0	4.2	1.4
VIOLETv2	VSWT	3.1	4.3	1.3
Temp[Swin]	SWT	4.9	6.6	2.3
Temp[CLIP]	ViT-B	6.1	8.3	3.7
Temp[BLIP]	ViT-B	6.9	10.0	4.5
FrozenBiLM	ViT-L	7.1	10.0	4.4
IGV	ResNet	14.0	19.8	9.6
TGB	OF+CNN	19.9	23.3	11.2

Table 5: Comparison results of Temporal Question Grounding task on NEXT-GQA (Xiao et al., 2023b).

509 cal flow improves from 43.84 to 53.67 (a relative
510 increase of 22.42%). indicating that optical flow
511 features can reduce the temporal information loss
512 caused by the sampling strategy.

513 **Analysis of Pluggable MLLMs** We substitute
514 the BLIP2 with three popular types of MLLMs,
515 mainly encoder-based models, *i.e.*, VIOLET (Fu
516 et al., 2021) as a representative of video-language
517 models, ALBEF (Li et al., 2021) as an image-
518 language model, SINGULARITY (Lei et al., 2022)
519 as a pre-trained model on a single frame of video
520 and image corpus. It’s noteworthy that we did not
521 incorporate the learned optical flow feature into
522 these MLLMs’ input. In this part, we also apply
523 all the experiments on AGQA 2.0 dataset. Table 1
524 (ALBEF + TGB, VIOLET + TGB, SINGULAR-
525 ITY + TGB) validates the efficacy of our TGB
526 and the versatility of our framework. On average,
527 the solver achieves a 3.68% accuracy improvement
528 after replacing the uniform sampled frames with
529 keyframes extracted by the TGB. These results con-
530 sistentlly demonstrate the effectiveness of our TGB
531 framework across various MLLMs.

532 **Generality of TGB** To demonstrate the gen-
533 erality of our approach, we applied our model to
534 visual instruction datasets (Lin et al., 2023). We
535 also adapted the LLM using LoRA (Hu et al.,
536 2022) to ensure a fair comparison with current
537 SOTA methods. As shown in Table 4, our method’s
538 performance on the videoQA dataset in a zero-
539 shot setting is presented. Unlike VideoLLaVA, our
540 method was not pretrained on additional datasets;
541 it was only fine-tuned on the same visual instruction
542 datasets. The results demonstrate that our method
543 can match the performance of the latest state-of-
544 the-art (SOTA) MLLMs, even though the LLM of
545 our model is less than half their size. This high-
546 lights the considerable promise of our framework
547 in this domain.

Model	Object-relation	Relation-action	Object-action	Others	All
TGB	62.27	51.74	66.09	57.04	61.45
w/o optical flow	59.13	15.06	50.79	51.29	55.00
w/ fixed bridge	62.28	47.84	50.68	53.47	59.88
w/ uniform sampling	53.72	48.64	62.10	50.68	54.00
w/ zero-shot	23.60	17.09	29.37	40.72	25.54

Table 6: **Ablation study of our method on reasoning questions from AGQA 2.0.** We list the major outputs of complicated relationships and summarize the rest; see *SM* for complete results.

4.2 Temporal Question Grounding on Video

Setup We use the Temporal Question Grounding on Video (TQGV) dataset NExT-GQA (Xiao et al., 2023a) to evaluate the efficacy of our TGB. We select a wide range of MLLMs as baselines: VGT (Xiao et al., 2022), Temp (Buch et al., 2022; Xiao et al., 2023b), FrozenBiLM (Yang et al., 2022), IGV (Li et al., 2022), and SeViLA (Yu et al., 2023). These baseline models encompass a variety of architectures, text encoders, and vision encoders. In contrast, our method does not depend on heavy offline vision feature extractors. We obtain the optical flow using a fixed RAFT (Teed and Deng, 2020), a model with only 5.26 million parameters. This comparison highlights the efficiency and simplicity of our approach.

Main Results and Analysis As shown in Table 5, our method outperforms baselines using additional feature extractors (Ren et al., 2015; Liu et al., 2021b,a; Radford et al., 2021). Our TGB with optical flow effectively learns temporal priors for video-language tasks. We suggest that discrete frames may introduce irrelevant visual cues, increasing the computational load for temporal learning. Despite this, all methods struggle with temporal grounding, with most mIoU values under 0.20, indicating a significant gap in current temporal modeling. Conversely, our TGB’s temporal features could mitigate these issues. We posit that our approach could significantly advance spatial-temporal research for extended videos. Qualitative results are presented in Appendix G.

4.3 Ablation Study

We apply ablation study on TGB to investigate the effects of our joint training framework. All the experiments are performed on AGQA 2.0 (Grunde-McLaughlin et al., 2021). As shown in Table 6, the framework incorporating motion feature significantly improved performance by 11.72%, underscoring its effectiveness in tackling spatial-

Model	FLOPs (GFLOPs) ↓	MACs (GMACs) ↓	Acc. ↑
BLIP2 (ViT-G)	2,705	1,350	69.6
Sevila (ViT-G)	13,720	14,357	71.5
TGB (ViT-G)	19,620	9,840	72.3
TGB (OFs)	2,950	1,474	72.1

Table 7: **Computational Efficiency of TGB.**

temporal problems. We also found that fixing the pre-trained TGB during training notably affected performance on temporal questions like “Relation-action”, suggesting that joint training can further optimize the bridge. Lastly, comparing with zero-shot and fine-tuned BLIP2 (Li et al., 2023b) with uniformly-sampled frames, our method shows significant improvements, demonstrating its overall effectiveness. In Appendix C.1, we provide detailed ablation study about the TGB-augmented models.

4.4 Time Efficiency

We evaluated the average inference time efficiency of our method against BLIP2 using calcflops (xiaoju ye, 2023) on the NExT-QA dataset, as shown in Table 7. Our method outperformed the current SOTA model SeViLa, which uses the LLM to select keyframes, both in terms of performance and efficiency. While replacing the OFs with features from ViT-G (Zhai et al., 2021) resulted in minor improvements, it significantly increased computation costs due to the offline feature extractor. Compared to BLIP2, our method required minimal additional computation. The major computation costs were associated with the LLMs from BLIP2 and the offline feature extractor. We believe our method strikes a balance between being effective and computationally efficient. Further details on the composition of the inference time of TGB are provided in *SM*. In addition, we investigate the composition of inference time of TGB and offline demo in Appendix B.

5 Conclusion

In this work, we propose a pluggable framework TGB for long Video-Language Understanding tasks, which comprises a TGB and a spatial prompt solver to combine spatial-temporal-language alignment and temporal grounding. Experiments on long-form video question answering and temporal question grounding on video demonstrate a consistent improvement over various types of MLLMs. Comprehensive analysis verifies the effectiveness, efficiency, and generality of our framework.

630 **Limitations**

631 Our study has one primary limitation: *i.e.* **Limited**
632 **Temporal Grounding Capability** As shown in
633 Section 4.2, our method outperforms existing ap-
634 proaches but still has restricted temporal grounding
635 capabilities, a common issue in current research.
636 We suspect that this limitation may be due to the
637 constraints of the lightweight 6-layer transformer-
638 based TGB. In future work, we aim to enhance this
639 aspect of our method without sacrificing efficiency.

640 **Ethics Statement and Broad Impact**

641 **References**

642 Yutong Bai, Xinyang Geng, Karttikeya Mangalam, Amir
643 Bar, Alan L. Yuille, Trevor Darrell, Jitendra Malik,
644 and Alexei A. Efros. 2023. Sequential modeling
645 enables scalable learning for large vision models.
646 *CoRR*, abs/2312.00785.

647 Max Bain, Arsha Nagrani, Gül Varol, and Andrew Zis-
648 serman. 2021. Frozen in time: A joint video and
649 image encoder for end-to-end retrieval. *International*
650 *Conference on Computer Vision (ICCV)*, pages 1708–
651 1718.

652 S. Buch, Cristobal Eyzaguirre, Adrien Gaidon, Jiajun
653 Wu, Li Fei-Fei, and Juan Carlos Niebles. 2022. Re-
654 visiting the “video” in video-language understanding.
655 *Conference on Computer Vision and Pattern Recog-
656 nition (CVPR)*, pages 2907–2917.

657 João Carreira and Andrew Zisserman. 2017. Quo vadis,
658 action recognition? A new model and the kinetics
659 dataset. In *Conference on Computer Vision and Pat-
660 tern Recognition (CVPR)*, pages 4724–4733. IEEE
661 Computer Society.

662 Yang Chen, Hexiang Hu, Yi Luan, Haitian Sun, Soravit
663 Changpinyo, Alan Ritter, and Ming-Wei Chang. 2023.
664 Can pre-trained vision and language models answer
665 visual information-seeking questions? *ArXiv*.

666 Wenliang Dai, Junnan Li, Dongxu Li, Anthony
667 Meng Huat Tiong, Junqi Zhao, Weisheng Wang,
668 Boyang Li, Pascale Fung, and Steven Hoi. 2023. **In-**
669 **structblip: Towards general-purpose vision-language**
670 **models with instruction tuning**.

671 Jacob Devlin, Ming-Wei Chang, Kenton Lee, and
672 Kristina Toutanova. 2019. Bert: Pre-training of deep
673 bidirectional transformers for language understand-
674 ing. In *North American Chapter of the Association*
675 *for Computational Linguistics: Human Language*
676 *Technologies (NAACL-HLT)*.

677 Danny Driess, Fei Xia, Mehdi S. M. Sajjadi, Corey
678 Lynch, Aakanksha Chowdhery, Brian Ichter, Ayzan
679 Wahid, Jonathan Tompson, Quan Vuong, Tianhe
680 Yu, Wenlong Huang, Yevgen Chebotar, Pierre Ser-
681 manet, Daniel Duckworth, Sergey Levine, Vincent

Vanhoucke, Karol Hausman, Marc Toussaint, Klaus
Greff, Andy Zeng, Igor Mordatch, and Pete Florence.
2023. **Palm-e: An embodied multimodal language**
682 **model**. 683 684 685

Chenyou Fan, Xiaofan Zhang, Shu Zhang, Wensheng
Wang, Chi Zhang, and Heng Huang. 2019. Heteroge-
neous memory enhanced multimodal attention model
for video question answering. *Conference on Com-
puter Vision and Pattern Recognition (CVPR)*, pages
1999–2007. 686 687 688 689 690 691

Christoph Feichtenhofer, Haoqi Fan, Jitendra Malik,
and Kaiming He. 2019. Slowfast networks for video
recognition. In *International Conference on Com-
puter Vision (ICCV)*, pages 6201–6210. IEEE. 692 693 694 695

Runyang Feng, Yixing Gao, Xueqing Ma, Tze Ho El-
den Tse, and Hyung Jin Chang. 2023. Mutual
information-based temporal difference learning for
human pose estimation in video. In *Conference on*
696 *Computer Vision and Pattern Recognition (CVPR)*,
697 pages 17131–17141. 698 699 700 701

Chaoyou Fu, Peixian Chen, Yunhang Shen, Yulei Qin,
Mengdan Zhang, Xu Lin, Zhenyu Qiu, Wei Lin, Jin-
rui Yang, Xiawu Zheng, Ke Li, Xing Sun, and Ron-
grong Ji. 2023. Mme: A comprehensive evaluation
benchmark for multimodal large language models.
ArXiv. 702 703 704 705 706 707

Tsu-Jui Fu, Linjie Li, Zhe Gan, Kevin Lin,
William Yang Wang, Lijuan Wang, and Zicheng
Liu. 2021. Violet : End-to-end video-language
transformers with masked visual-token modeling.
ArXiv, abs/2111.12681. 708 709 710 711 712

Difei Gao, Luowei Zhou, Lei Ji, Linchao Zhu, Yi Yang,
and Mike Zheng Shou. 2023a. MIST : Multi-modal
iterative spatial-temporal transformer for long-form
video question answering. In *Conference on Com-
puter Vision and Pattern Recognition (CVPR)*, pages
14773–14783. IEEE. 713 714 715 716 717 718

Peng Gao, Jiaming Han, Renrui Zhang, Ziyi Lin, Shijie
Geng, Aojun Zhou, Wei Zhang, Pan Lu, Conghui He,
Xiangyu Yue, Hongsheng Li, and Yu Qiao. 2023b.
Llama-adapter v2: Parameter-efficient visual instruc-
696 **tion model**. 719 720 721 722 723

Madeleine Grunde-McLaughlin, Ranjay Krishna, and
Maneesh Agrawala. 2021. Agqa: A benchmark for
compositional spatio-temporal reasoning. In *Confer-
ence on Computer Vision and Pattern Recognition*
696 *(CVPR)*. 724 725 726 727 728

Bo He, Hengduo Li, Young Kyun Jang, Menglin Jia,
Xuefei Cao, Ashish Shah, Abhinav Shrivastava,
and Ser-Nam Lim. 2024. MA-LMM: memory-
augmented large multimodal model for long-term
video understanding. *CoRR*, abs/2404.05726. 729 730 731 732 733

Lisa Anne Hendricks, Oliver Wang, Eli Shechtman,
Josef Sivic, Trevor Darrell, and Bryan C. Russell.
2017. Localizing moments in video with natural lan-
guage. *International Conference on Computer Vision*
696 *(ICCV)*, pages 5804–5813. 734 735 736 737 738

739	Edward J. Hu, Yelong Shen, Phillip Wallis, Zeyuan Allen-Zhu, Yuanzhi Li, Shean Wang, Lu Wang, and Weizhu Chen. 2022. Lora: Low-rank adaptation of large language models. In <i>International Conference on Learning Representations (ICLR)</i> . OpenReview.net.	792	Jie Lei, Linjie Li, Luowei Zhou, Zhe Gan, Tamara L. Berg, Mohit Bansal, and Jingjing Liu. 2021. Less is more: Clipbert for video-and-language learning via sparse sampling. <i>Conference on Computer Vision and Pattern Recognition (CVPR)</i> , pages 7327–7337.	793
740		794		795
741		796		797
742				798
743				799
744				800
745	Shaohan Huang, Li Dong, Wenhui Wang, Yaru Hao, Saksham Singhal, Shuming Ma, Tengchao Lv, Lei Cui, Owais Khan Mohammed, Barun Patra, Qiang Liu, Kriti Aggarwal, Zewen Chi, Johan Bjorck, Vishrav Chaudhary, Subhojit Som, Xia Song, and Furu Wei. 2023. Language is not all you need: Aligning perception with language models .			801
746				802
747				803
748				804
749				805
750				806
751				807
752	Boyuan Jiang, MengMeng Wang, Weihao Gan, Wei Wu, and Junjie Yan. 2019. Stm: Spatiotemporal and motion encoding for action recognition. In <i>Proceedings of the IEEE/CVF International Conference on Computer Vision</i> , pages 2000–2009.			808
753				809
754				810
755				811
756				812
757	Pin Jiang and Yahong Han. 2020. Reasoning with heterogeneous graph alignment for video question answering. In <i>AAAI Conference on Artificial Intelligence (AAAI)</i> , pages 11109–11116. AAAI Press.			813
758				814
759				815
760				816
761	Zhuolin Jiang, Viktor Rozgic, and Sancar Adali. 2017. Learning spatiotemporal features for infrared action recognition with 3d convolutional neural networks. In <i>Conference on Computer Vision and Pattern Recognition (CVPR)</i> , pages 309–317. IEEE Computer Society.			817
762				818
763				819
764				820
765				821
766				822
767	Bruno Korbar, Yongqin Xian, Alessio Tonioni, Andrew Zisserman, and Federico Tombari. 2023. Text-conditioned resampler for long form video understanding. <i>CoRR</i> , abs/2312.11897.			823
768				824
769				825
770				826
771	Ranjay Krishna, Kenji Hata, Frederic Ren, Li Fei-Fei, and Juan Carlos Niebles. 2017. Dense-captioning events in videos. <i>International Conference on Computer Vision (ICCV)</i> .			827
772				828
773				829
774				830
775	Max Ku, Tianle Li, Kai Zhang, Yujie Lu, Xingyu Fu, Wenwen Zhuang, and Wenhui Chen. 2023. Imagenhub: Standardizing the evaluation of conditional image generation models. <i>ArXiv</i> .			831
776				832
777				833
778				834
779	Thao Minh Le, Vuong Le, Svetha Venkatesh, and Truyen Tran. 2020. Hierarchical conditional relation networks for video question answering. In <i>Conference on Computer Vision and Pattern Recognition (CVPR)</i> , pages 9969–9978. Computer Vision Foundation / IEEE.			835
780				836
781				837
782				838
783				839
784				840
785	Jie Lei, Tamara L. Berg, and Mohit Bansal. 2022. Revealing single frame bias for video-and-language learning. <i>ArXiv</i> , abs/2206.03428.			841
786				842
787				843
788	Jie Lei, Tamara Lee Berg, and Mohit Bansal. Detecting moments and highlights in videos via natural language queries. In <i>Advances in Neural Information Processing Systems (NeurIPS)</i> .			844
789				845
790				846
791				847
				848
				849
				850
				851
				852
				853
				854
				855
				856
				857
				858
				859
				860
				861
				862
				863
				864
				865
				866
				867
				868
				869
				870
				871
				872
				873
				874
				875
				876
				877
				878
				879
				880
				881
				882
				883
				884
				885
				886
				887
				888
				889
				890
				891
				892
				893
				894
				895
				896
				897
				898
				899
				900
				901
				902
				903
				904
				905
				906
				907
				908
				909
				910
				911
				912
				913
				914
				915
				916
				917
				918
				919
				920
				921
				922
				923
				924
				925
				926
				927
				928
				929
				930
				931
				932
				933
				934
				935
				936
				937
				938
				939
				940
				941
				942
				943
				944
				945
				946
				947
				948
				949
				950
				951
				952
				953
				954
				955
				956
				957
				958
				959
				960
				961
				962
				963
				964
				965
				966
				967
				968
				969
				970
				971
				972
				973
				974
				975
				976
				977
				978
				979
				980
				981
				982
				983
				984
				985
				986
				987
				988
				989
				990
				991
				992
				993
				994
				995
				996
				997
				998
				999
				1000

846	Ze Liu, Yutong Lin, Yue Cao, Han Hu, Yixuan Wei,	Shuhuai Ren, Linli Yao, Shicheng Li, Xu Sun, and	902
847	Zheng Zhang, Stephen Lin, and Baining Guo. 2021a.	Lu Hou. 2023. Timechat: A time-sensitive multi-	903
848	Swin transformer: Hierarchical vision transformer	modal large language model for long video under-	904
849	using shifted windows. In <i>International Conference</i>	standing. <i>CoRR</i> , abs/2312.02051.	905
850	on Computer Vision (ICCV).		
851	Ze Liu, Jia Ning, Yue Cao, Yixuan Wei, Zheng Zhang,	Xindi Shang, Donglin Di, Junbin Xiao, Yu Cao, Xun	906
852	Stephen Lin, and Han Hu. 2021b. Video swin trans-	Yang, and Tat-Seng Chua. 2019. Annotating objects	907
853	former. <i>Conference on Computer Vision and Pattern</i>	and relations in user-generated videos. In <i>Proceed-</i>	908
854	<i>Recognition (CVPR)</i> , pages 3192–3201.	<i>ings of the 2019 on International Conference on Mul-</i>	909
		<i>timedia Retrieval</i> , pages 279–287. ACM.	910
855	Pan Lu, Swaroop Mishra, Tanglin Xia, Liang Qiu, Kai-	Enxin Song, Wenhao Chai, Guanhong Wang, Yucheng	911
856	Wei Chang, Song-Chun Zhu, Oyvind Tafjord, Peter	Zhang, Haoyang Zhou, Feiyang Wu, Xun Guo,	912
857	Clark, and Ashwin Kalyan. 2022. Learn to explain:	Tian Ye, Yan Lu, Jenq-Neng Hwang, and Gaoang	913
858	Multimodal reasoning via thought chains for science	Wang. 2023. Moviechat: From dense token to	914
859	question answering. <i>Advances in Neural Information</i>	sparse memory for long video understanding. <i>CoRR</i> ,	915
860	<i>Processing Systems (NeurIPS)</i> , 35:2507–2521.	abs/2307.16449.	916
861	Chenyang Lyu, Minghao Wu, Longyue Wang, Xinting	Jianlin Su, Yu Lu, Shengfeng Pan, Ahmed Murtadha,	917
862	Huang, Bingshuai Liu, Zefeng Du, Shuming Shi, and	Bo Wen, and Yunfeng Liu. 2021. <i>Roformer: En-</i>	918
863	Zhaopeng Tu. 2023. Macaw-llm: Multi-modal lan-	hanced transformer with rotary position embedding.	919
864	guage modeling with image, audio, video, and text		
865	integration.	Dídac Surís, Sachit Menon, and Carl Vondrick. 2023.	920
		<i>Vipergpt: Visual inference via python execution for</i>	921
866	Fan Ma, Xiaojie Jin, Heng Wang, Yuchen Xian, Jiashi	reasoning.	922
867	Feng, and Yi Yang. 2023. Vista-llama: Reliable video		
868	narrator via equal distance to visual tokens. <i>CoRR</i> ,	Zachary Teed and Jia Deng. 2020. <i>Raft: Recurrent all-</i>	923
869	abs/2312.08870.	pairs field transforms for optical flow. <i>Lecture Notes</i>	924
		<i>in Computer Science</i> , page 402–419.	925
870	Muhammad Maaz, Hanoona Rasheed, Salman Khan,	Bart Thomee, David A Shamma, Gerald Friedland, Ben-	926
871	and Fahad Shahbaz Khan. 2023. <i>Video-chatgpt: To-</i>	jamin Elizalde, Karl Ni, Douglas Poland, Damian	927
872	<i>wards detailed video understanding via large vision</i>	Borth, and Li-Jia Li. 2016. Yfcc100m: The new	928
873	<i>and language models.</i>	data in multimedia research. <i>Communications of the</i>	929
		<i>ACM</i> , 59(2):64–73.	930
874	Karttikeya Mangalam, Raiymbek Akshulakov, and Ji-	Zhan Tong, Yibing Song, Jue Wang, and Limin	931
875	tendra Malik. 2023. Egoschema: A diagnostic bench-	Wang. 2022. Videomae: Masked autoencoders are	932
876	mark for very long-form video language understand-	data-efficient learners for self-supervised video pre-	933
877	ing. In <i>Advances in Neural Information Processing</i>	training. In <i>Advances in Neural Information Process-</i>	934
878	<i>Systems 36: Annual Conference on Neural Informa-</i>	<i>ing Systems (NeurIPS)</i> .	935
879	<i>tion Processing Systems 2023, NeurIPS 2023, New</i>		
880	<i>Orleans, LA, USA, December 10 - 16, 2023.</i>	Ashish Vaswani, Noam Shazeer, Niki Parmar, Jakob	936
881	Tomas Pfister, James Charles, and Andrew Zisserman.	Uszkoreit, Llion Jones, Aidan N Gomez, Łukasz	937
882	2015. Flowing convnets for human pose estimation	Kaiser, and Illia Polosukhin. 2017. Attention is all	938
883	in videos. In <i>International Conference on Computer</i>	you need. In <i>Advances in Neural Information Pro-</i>	939
884	<i>Vision (ICCV)</i> , pages 1913–1921.	<i>cessing Systems (NeurIPS)</i> , pages 6000–6010.	940
885	Long Qian, Juncheng Li, Yu Wu, Yaobo Ye, Hao Fei,	Alex Jinpeng Wang, Yixiao Ge, Rui Yan, Ge Yuying,	941
886	Tat-Seng Chua, Yueting Zhuang, and Siliang Tang.	Xudong Lin, Guanyu Cai, Jianping Wu, Ying Shan,	942
887	2024. Momentor: Advancing video large language	Xiaohu Qie, and Mike Zheng Shou. 2023. All in one:	943
888	model with fine-grained temporal reasoning. <i>CoRR</i> ,	Exploring unified video-language pre-training. <i>Con-</i>	944
889	abs/2402.11435.	<i>ference on Computer Vision and Pattern Recognition</i>	945
		<i>(CVPR)</i> .	946
890	Alec Radford, Jong Wook Kim, Chris Hallacy, Aditya	Chenfei Wu, Shengming Yin, Weizhen Qi, Xiaodong	947
891	Ramesh, Gabriel Goh, Sandhini Agarwal, Girish Sas-	Wang, Zecheng Tang, and Nan Duan. 2023. <i>Visual</i>	948
892	try, Amanda Askell, Pamela Mishkin, Jack Clark,	<i>chatgpt: Talking, drawing and editing with visual</i>	949
893	Gretchen Krueger, and Ilya Sutskever. 2021. <i>Learn-</i>	<i>chatgpt: Talking, drawing and editing with visual</i>	950
894	<i>ing transferable visual models from natural language</i>	<i>foundation models.</i>	
895	<i>supervision.</i> In <i>International Conference on Machine</i>	Junbin Xiao, Xindi Shang, Angela Yao, and Tat-Seng	951
896	<i>Learning (ICML)</i> , volume 139 of <i>Proceedings of Ma-</i>	Chua. 2021. Next-qa: Next phase of question-	952
897	<i>chine Learning Research</i> , pages 8748–8763. PMLR.	answering to explaining temporal actions. <i>Confer-</i>	953
898	Shaoqing Ren, Kaiming He, Ross B. Girshick, and Jian	<i>ence on Computer Vision and Pattern Recognition</i>	954
899	Sun. 2015. Faster r-cnn: Towards real-time object	<i>(CVPR)</i> , pages 9772–9781.	955
900	detection with region proposal networks. 39:1137–		
901	1149.		

956	Junbin Xiao, Angela Yao, Yicong Li, and Tat-Seng Chua. 2023a. Can I trust your answer? visually grounded video question answering. <i>CoRR</i> , abs/2309.01327.	Youngjae Yu, Jongseok Kim, and Gunhee Kim. 2018. A joint sequence fusion model for video question answering and retrieval. <i>European Conference on Computer Vision (ECCV)</i> .	1008
957			1009
958			1010
959			1011
960	Junbin Xiao, Angela Yao, Yicong Li, and Tat-Seng Chua. 2023b. Can i trust your answer? visually grounded video question answering. <i>ArXiv</i> .	Zhou Yu, D. Xu, Jun Yu, Ting Yu, Zhou Zhao, Yueting Zhuang, and Dacheng Tao. 2019. Activitynet-qa: A dataset for understanding complex web videos via question answering. <i>AAAI Conference on Artificial Intelligence (AAAI)</i> .	1012
961			1013
962			1014
963	Junbin Xiao, Pan Zhou, Tat-Seng Chua, and Shuicheng Yan. 2022. Video graph transformer for video question answering. In <i>European Conference on Computer Vision (ECCV)</i> , volume 13696 of <i>Lecture Notes in Computer Science</i> , pages 39–58. Springer.	Xiaohua Zhai, Alexander Kolesnikov, Neil Houlsby, and Lucas Beyer. 2021. Scaling vision transformers. <i>Conference on Computer Vision and Pattern Recognition (CVPR)</i> , pages 1204–1213.	1015
964			1016
965			1017
966			1018
967			1019
968	xiaoju ye. 2023. calflops: a flops and params calculate tool for neural networks in pytorch framework .	Dingwen Zhang, Guangyu Guo, Dong Huang, and Junwei Han. 2018. Poseflow: A deep motion representation for understanding human behaviors in videos. In <i>Proceedings of the IEEE Conference on Computer Vision and Pattern Recognition</i> , pages 6762–6770.	1020
969			1021
970	Saining Xie, Ross B. Girshick, Piotr Dollár, Zhuowen Tu, and Kaiming He. 2017. Aggregated residual transformations for deep neural networks. In <i>Conference on Computer Vision and Pattern Recognition (CVPR)</i> , pages 5987–5995. IEEE Computer Society.	Hang Zhang, Xin Li, and Lidong Bing. 2023a. Video-llama: An instruction-tuned audio-visual language model for video understanding .	1022
971			1023
972			1024
973			1025
974			1026
975	D. Xu, Zhou Zhao, Jun Xiao, Fei Wu, Hanwang Zhang, Xiangnan He, and Yueting Zhuang. 2017. Video question answering via gradually refined attention over appearance and motion. <i>Association for Computing Machinery's Annual Conference on Multimedia (ACM MM)</i> .	Kai Zhang, Lingbo Mo, Wenhui Chen, Huan Sun, and Yu Su. 2023b. Magicbrush: A manually annotated dataset for instruction-guided image editing. <i>ArXiv</i> .	1027
976			1028
977			1029
978			1030
979			1031
980			1032
981	Haiyang Xu, Qinghao Ye, Ming Yan, Yaya Shi, Jiabo Ye, Yuanhong Xu, Chenliang Li, Bin Bi, Qi Qian, Wei Wang, Guohai Xu, Ji Zhang, Songfang Huang, Fei Huang, and Jingren Zhou. 2023. mplug-2: A modularized multi-modal foundation model across text, image and video .	Deyao Zhu, Jun Chen, Xiaoqian Shen, Xiang Li, and Mohamed Elhoseiny. 2023. Minigtpt-4: Enhancing vision-language understanding with advanced large language models .	1033
982			1034
983			1035
984			
985			
986			
987	Jun Xu, Tao Mei, Ting Yao, and Yong Rui. 2016. Msr-vtt: A large video description dataset for bridging video and language. <i>Conference on Computer Vision and Pattern Recognition (CVPR)</i> , pages 5288–5296.		
988			
989			
990			
991	Zhiyang Xu, Ying Shen, and Lifu Huang. 2022. Multi-instruct: Improving multi-modal zero-shot learning via instruction tuning. In <i>Annual Meeting of the Association for Computational Linguistics (ACL)</i> .		
992			
993			
994			
995	Antoine Yang, Antoine Miech, Josef Sivic, Ivan Laptev, and Cordelia Schmid. 2021. Just ask: Learning to answer questions from millions of narrated videos. In <i>Conference on Computer Vision and Pattern Recognition (CVPR)</i> , pages 1686–1697.		
996			
997			
998			
999			
1000	Antoine Yang, Antoine Miech, Josef Sivic, Ivan Laptev, and Cordelia Schmid. 2022. Zero-shot video question answering via frozen bidirectional language models. In <i>Advances in Neural Information Processing Systems (NeurIPS)</i> .		
1001			
1002			
1003			
1004			
1005	Shoubin Yu, Jaemin Cho, Prateek Yadav, and Mohit Bansal. 2023. Self-chained image-language model for video localization and question answering .		
1006			
1007			

Appendices

Table of Contents

A Self-Improvement Algorithm	13
B Inference Time Analysis	13
C More Analysis Experiments	13
C.1 Ablated TSP-augmented models	13
C.2 Influence of the number of frames on solver	14
C.3 Detailed Ablation Study Results	14
D Details of Multi-span Prediction	14
E Implementation Details	14
F Details of Datasets	14
F.1 Implementation Details of TGB on Downstream Tasks	15
F.2 Prompt for Multiple-choice Task on BLIP2	15
G Qualitative Studies on NExTGQA	15
H Qualitative Studies on AGQA 2.0	15

A Self-Improvement Algorithm

Algorithm 1 shows our self-improvement algorithm of automatically generating pseudo labels by the MLLM, which is used to optimize the TGB.

B Inference Time Analysis

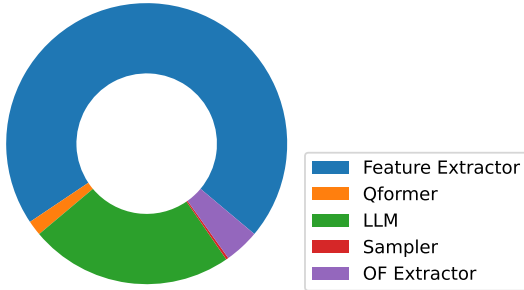


Figure 3: Inference time Analysis

We further investigate the composition of inference time of TGB on the NExT-QA dataset. We find most computation costs come from LLM and the

Algorithm 1: Pseudo Label Algorithm

Input: frames ($V = \{fr_1, fr_2, \dots, fr_T\}$), query (q), answer (a)

Output: temporal grounded span

```

scorebest ← 0
start ← 0
end ← T - 1
stack ← empty list
scores ← empty list
for fr in V do
  prediction = LLMMLLM(fr, q)
  scores.add(SIM(prediction, a))
end
for i in scores.length do
  while stack is not empty and
    stack.get(score.top) > score.get(i)
  do
    tmp = stack.pop()
    scoretmp = (i - stack.top - 1) ×
      score.get(tmp)
    if scoretmp > scorebest then
      scorebest = scoretmp
      start = 0
      end = i - 2
    else
      end
    end
  end
  stack.push(i)
end

```

offline feature extractor. Compared with other components, the computation cost is trivial, indicating the strong efficiency of our method. The offline demo is presented in the supplementary material.

C More Analysis Experiments

C.1 Ablated TSP-augmented models

TGB	MLLM	# of frames (Train)	# of frames (Infer.)	Acc.
OF	SING-17M	1	6	53.13
OF	SING-17M	1	1	51.36
OF	SING-17M	6	6	53.85
OF	SING-5M	1	6	51.10
Swin.	SING-17M	1	6	53.76

Table 8: Detailed Analysis on the TGB.

In Table 8, we analyzed TSP+SINGULARITY to evaluate the TSP-augmented paradigm. Our study revealed that increasing the number of frames dur-

ing inference improved performance by 3.4%, but further increases did not proportionally enhance results. We also found that MLLM benefits more from the sampling strategy when adequately pre-trained (*i.e.*, 17M denotes the model is pretrained on 17M video corpora). Additionally, we proposed two TGB variants, replacing optical flow with features extracted by the video SwinTransformer (Liu et al., 2021b) for pre-training. The comparable results suggest that our TSP can effectively reason over time without any prior perception information.

C.2 Influence of the number of frames on solver

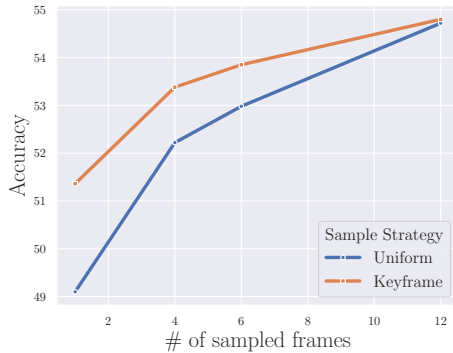


Figure 4: Further study on the number of sampled frames.

We trained the solver with different numbers of sampled frames. Results are shown in Figure 4. The fewer sampled frames the better performance of the keyframe strategy, and after a certain point, the uniform strategy performs close to the keyframe strategy. This is because the average duration of videos in AGQA is around 30 seconds, 12 frames are close to dense sampling which covers almost all visual cues. In other words, video-language tasks require bountiful frame inputs that have high computational complexity, but our method efficiently learns near-complete video information.

C.3 Detailed Ablation Study Results

	TGB	w/o Optical Flow	fixed TGB	Uniform Sample	Zero-Shot
Obj-rel	62.27	59.13	62.28	53.72	23.60
Rel-act	51.74	15.06	47.84	48.64	17.09
Obj-act	66.09	50.79	50.68	62.10	29.37
Superlative	53.67	59.79	52.12	43.84	28.39
Sequencing	60.11	35.04	49.43	55.94	48.79
Exists	60.85	60.92	60.96	55.14	48.79
Duration	36.99	26.48	40.18	40.39	26.99
Action	0.00	0.00	0.00	0.28	0.28
All	61.45	55.00	59.88	54.00	25.54

Table 9: Ablation study of our method on reasoning questions from AGQA 2.0 (Grunde-McLaughlin et al., 2021).

In Table 9, we demonstrate the details of the ablation study of TGB on AGQA 2.0. Specifically, we demonstrate the ablation study results of different question types.

D Details of Multi-span Prediction

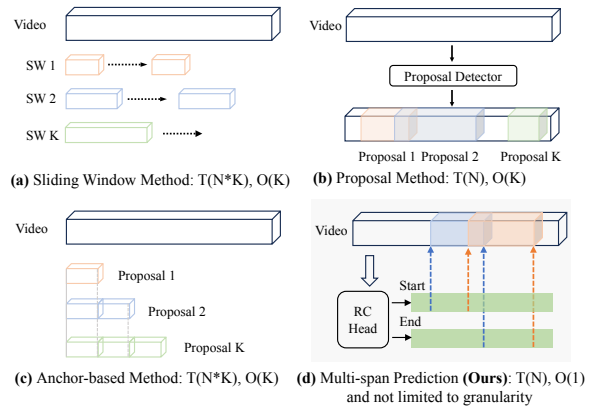


Figure 5: Comparison of multi-span RC prediction (d) and other methods (a-c) in terms of time and space complexity.

In Fig. 5, we compare our proposed multi-span reading comprehension prediction algorithm and other commonly used methods for temporal sentence grounding on video tasks, including the sliding window method, proposal method, and anchor-based method.

E Implementation Details

F Details of Datasets

Long-form VideoQA. AGQA is specially designed for compositional spatial-temporal reasoning¹ including 1,455,610/669,207 question answering for train/test splits. NEXTQA is a multiple choice VideoQA benchmark for causal, temporal,

¹We use AGQA 2.0 which has more balanced distributions.

1115
1116

and descriptive reasoning, including 52K questions.

1117
1118
1119
1120
1121
1122
1123

Temporal Question Grounding on Video. NExT-GQA is an extension of NExT-QA (Xiao et al., 2021) with 10.5K temporal grounding labels tied to questions, which contains 3,358/5,553 questions for val/test splits. We report mean Intersection over Union (mIoU), IoU@0.3, and IoU@0.5 as metrics following (Xiao et al., 2023a).

1124
1125

F.1 Implementation Details of TGB on Downstream Tasks

1126
1127
1128
1129
1130
1131
1132
1133
1134
1135
1136
1137
1138
1139
1140
1141
1142

The TGB is a 6-layer transformer with RoPE (Su et al., 2021). For TGB, We use BLIP2-flant5-xl (Li et al., 2023b) as TGB. For the TGB-augmented framework, we take three vision-language pre-training models as the solver: ALBEF (Li et al., 2021), SINGULARITY (Lei et al., 2022), and VIOLET (Fu et al., 2021) For the number of keyframes, we sample 4 frames for TGB and 6 frames for TGB-augmented methods to keep consistent with baselines. We take $K = 2$ for Gumbel-Softmax tricks in practice. We extract the dense optical flow from the video by RAFT (Teed and Deng, 2020). For the BLIP2-based model, the total trainable parameters are 195M, thus our framework is lightweight and can be easily adapted to any LLM. All the experiments are performed on NVIDIA A100 80G GPU.

1143
1144

F.2 Prompt for Multiple-choice Task on BLIP2

1145
1146
1147

Following (Yu et al., 2023), we construct additional prompts to adapt the generative model to the multiple-choice task.

Question: why did the boy pick up one present from the group of them and move to the sofa ?
Option A: share with the girl
Option B: approach lady sitting there
Option C: unwrap it
Option D: playing with toy train
Option E: gesture something
Considering the information presented in the frame, select the correct answer from the options.

Figure 6: Additional prompt for NExT-MC task

G Qualitative Studies on NExTGQA

1148



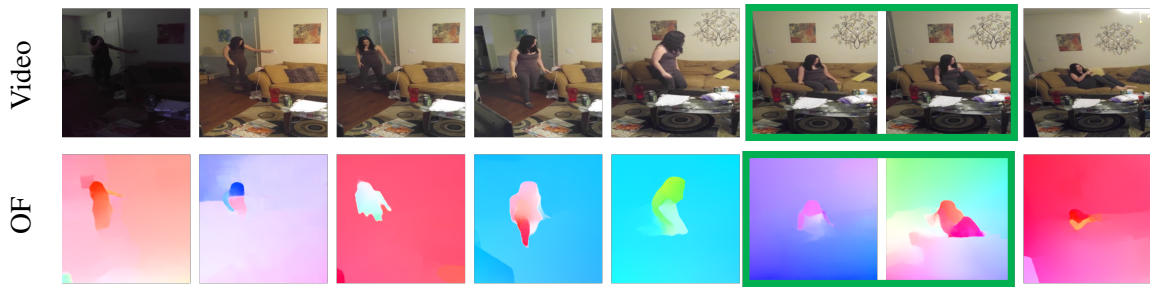
Figure 7: Qualitative results on temporal grounding

Fig. 7 presents two random outputs from TGB on the TQGV task. The first example demonstrates how our method can ground video using the semantic information from the question, specifically, the phrase "at the beginning". The second example demonstrates the efficacy of our method in temporal reasoning, as evidenced by the phrase "as she walked".

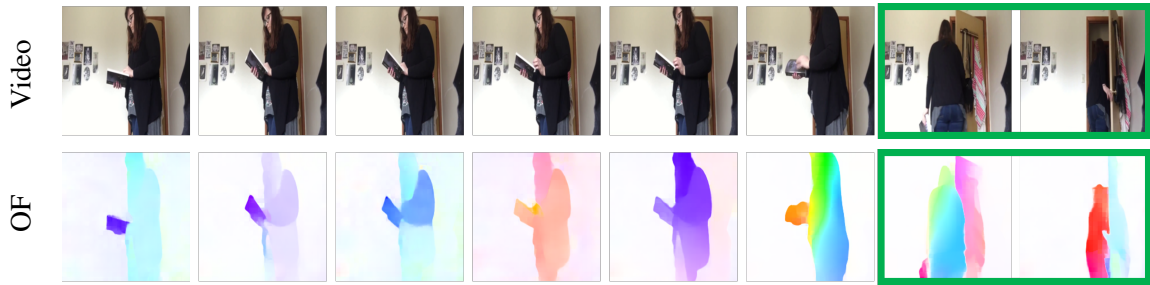
1149
1150
1151
1152
1153
1154
1155
1156

H Qualitative Studies on AGQA 2.0

1157



Question: Before holding a book but after sitting in a bed, what did they undress?
Ground Truth: shoe **TGB:** shoe **BLIP2:** dish **SEVILA:** clothes



Question: Which object did the person grasp after watching a book?
Ground Truth: doorknob **TGB:** doorknob **BLIP2:** NA **SEVILA:** doorway

Figure 8: Case Studies. OF: Optical Flow. Green and red boxes indicate correct and wrong keyframe predictions, respectively. In these cases, our method could correctly localize the keyframes and predict the right answer. “NA” indicates the BLIP2 can’t generate an answer hitting the answer vocabulary.



Question: Between putting a book somewhere and tidying something on the floor, which object were they undressing?
Prediction: shoe **Ground Truth:** clothes



Question: What was the person taking between putting a cup somewhere and holding a book?
Prediction: box **Ground Truth:** food

Figure 9: Filure Cases. OF: Optical Flow. Green and red boxes indicate correct and wrong keyframe predictions, respectively. For complicated situations involving more than one event, *e.g.*, “between putting a cup and holding a book”, our method could fail to localize the keyframes and thus print the wrong answer.